Mineral Res. Expl. Bull., 136, 1-16, 2008

MINING GEOLOGY OF THE GOLD OCCURRENCES RELATED TO THE ARSENOPYRITES OF İZMİR-ÖDEMİŞ REGION

Sinan AKISKA* , Taner ÜNLÜ* and İ. Sönmez SAYILI*

ABSTRACT.- This study presents the results of the mineralogical, petrographical and geochemical investigations of the gold bearing vein-like arsenopyrite occurrences and mica schist, amphibole schist and amphibolite host rocks cropping out in the close vicinities of Elmacıgediği, Zeytinlik, Yılanlıkale and Kemer regions in the northeast of Ödemiş, İzmir. All investigated areas are located in the Ödemiş submassif of the Menderes Massif which consist of schists, gneisses and amphibolites. These units are formed under the conditions of medium grade metamorphism. Garnet-biotite-amphibolite, amphibole schists and mica schists crop out in the study area. They are generally rich in biotite and/or muscovite and in some localities garnet. The amphibolites which are formed as lense-like bodies, are more than several hundreds of meters in length and several tens of meters in thickness and are aligned parallel to the schistosity of mica schists. Geochemical analyses have been carried out on 11 selected samples. In the major oxides versus SiO_2 diagrams, ores mica schists and amphibolites/amphibole schists plot in different areas. Very high positive correlation coefficients among Au-Ag-Sb-Bi and Se are held from the trace element data of 7 samples taken from Zeytinlik area in statistically evaluation. Ore microscopical studies indicate two different stages for ore mineralizations as syngenetic and postmetamorphic. Mineralizations are formed both related with elements of basic magmatic rocks carried by solutions into the sedimentary basin and afterwards, the elements related with more asidic solutions. Mineralizations are remobilized during and/or after the metamorphism of the region.

Key words: Menderes Massif, Ödemiş submassif, arsenopyrite, gold, İzmir

INTRODUCTION

Some deposits are especially observed in Precambrian aged Canadian Greenstone Belts in the world when gold deposits in metamorphic terranes are investigated (Strachan and Moffett 1985, Kuhns 1988, Sawkins 1990). It is possible to see gold deposits related to the metamorphic rocks, metamorphosed volcanic and/or ultramafic rocks, or the rocks over the metamorphic basement in the Menderes Massif, Çanakkale, Hatay and Kastamonu in Turkey (Önal et. al., 1986, Kayhan 1991, Aydal 2000).

73 gold occurrences as gold bearing arsenopyrite and quartz veins have been found out during the detailed studies of MTA General Directorate carried out around Ödemiş and Çine Submassifs of Menderes Massif and Uşak and Eşme provinces at the eastern part of the Massif (Dilek and Kayhan 1987, Kayhan 1991). Gold and spatially tungsten have been determined in some analyses at Mursallı, Zeytinlik, Höyük Tepe, Elmacıgediği, Yılanlıkale, Akçakmakgediği, Küçük Avulcuk and Kemer occurrences around Ödemiş in Ödemiş Submassif (Dilek and Kayhan 1987, Kayhan 1991, Andiç 1992, Gonca 1992).

Scheelite and arsenopyrites occur in metamorphic rocks ,especially in amphibolites, in the region. Arsenopyrites form in schists in some regions and in amphibolites in other regions. Veinlike arsenopyrite mineralizations are followed sometimes in coincidence with the schistosity of schists and in some places cutting the schistosity planes. The thicknesses of the veins vary between a few cm's and 10 cm, while the length of veins reach up to 70 meters.

* Ankara Üniversitesi Mühendislik Fakültesi Jeoloji Mühendisliği Bölümü, 06100 Tandoğan/ANKARA
e-mail : akiska@eng.ankara.edu.tr, tunlu@eng.ankara.edu.tr, sayili@eng.ankara.edu.tr

The origin of the gold mineralizations in both arsenopyrite and quartz veins in the Massif are interpreted as either related with hydrothermal veins or fracture fillings due to hydrothermal mobilizations from stratabound ore levels of sedimentary origin which are affected from Varistic and Alpine Orogeny (Uzkut 1977, Çağatay and Eyüpoğlu 1979, Dilek and Kayhan 1987, Kayhan 1991, Andiç 1992, Gonca 1992). In this study, the origin of the mineralizations will be evaluated according to the collected geological data.

GENERAL GEOLOGY, MINERALOGY AND PETROGRAPHY

Geological, mineralogical and petrographical investigations are carried out in Elmacıgediği, Zeytinlik, and Yılanlıkale districts at the İzmir L20 a4 sheet. Since Kemer and Yılanlıkale districts are close settlements, these two occurrences will be interpreted together (Figure 1).

Elmacıgediği Area

This area is located 12 km northwest of Gölcük, east of Ödemiş-Bozdağ road. Garnet-mica schists and amphibolites crop out at the study area. Mica schists are generally brown and yellowish in colors. Schistosity of mica schists show strikes of E-W in general and rarely NW-SE and dip directions of S or SW with 40 to 70 degrees. The strikes of arsenopyrite bearing veins are E-W, NNW-SSE and N-S. Main minerals in mica schists are generally sillimanite, kyanite, biotite, muscovite, quartz, garnet and staurolite. Biotites are altered to hydrobiotites especially in close parts to the ore bearing zones. Some biotites have zircon inclusions (Plate I - Figure 1).

Lens-shaped amphibolites have more than a few hundred meters in lenghts and a few ten of meters in thicknesses. Greenish to blackish colored amphibolites contain coarse-grained minerals which are characterized by amphiboles, garnets, biotites and plagioclases. Microscopic investigations indicate that amphiboles are hornblendes according to their greenish pleochroisms. They display hypidioblastic to xenoblastic textures (Plate I - Figure 2). Xenoblastic plagioclases have polysentetic twinnings. Opaque mineral inclusions are common in the hypidioblastic and idioblastic garnets which are often developed in secondary fractures. Hypidioblastic biotite porphyroblasts exhibit brown pleochroisms. Quartz, muscovite, sphene, rutile and opaque minerals are also observed in thin sections.

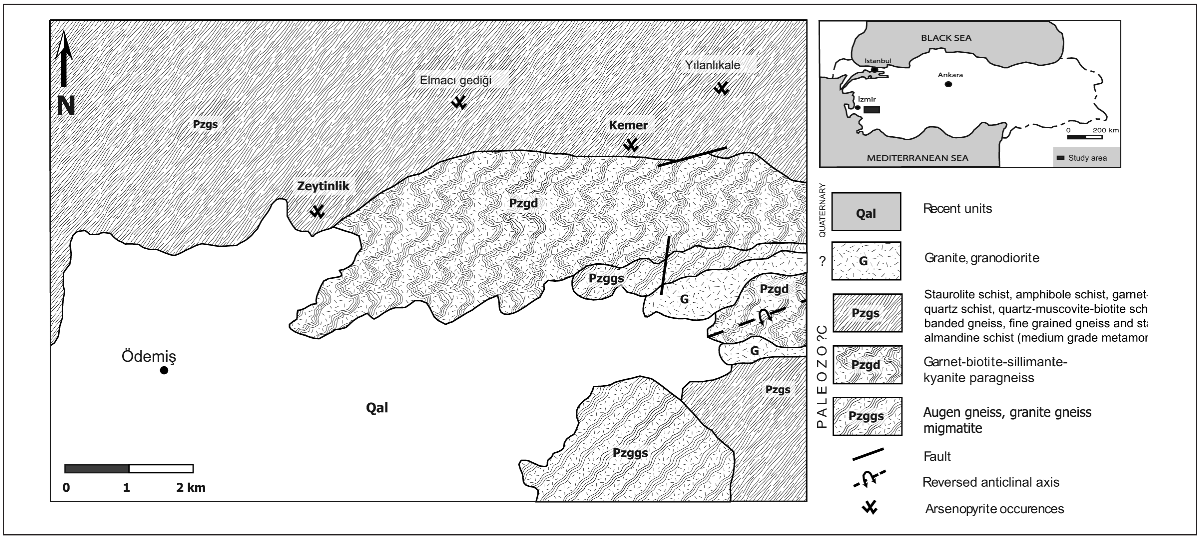

Figure 1- Regional geologic map of the investigated area (modified from Dilek and Kayhan, 1987).

Zeytinlik Area

This area is located at NE of Zeytinlik village which is 4 km away from Ödemiş in NE direction and on Gölcük road.

Massive arsenopyrite veins and veinlets are generally concordant with the schistosity of the biotite-quartz-muscovite-garnet schists at this area. The strike and dip of the veins are N62E / 46NW. The thicknesses of massive arsenopyrite veins vary between 10-15 cm and their lengths are in a few meters. In another location of the Zeytinlik area, a quartz lens with a 2,5 meter thickness is also observed which includes fine grained arsenopyrite disseminations. East of this location, arsenopyrite mineralizations which cut the schistosity of the rocks, crop out varying up to 10 cm thicknesses.

According to previous geological and petrographical studies, mica schist are classified as staurolite and garnet bearing kyanite-mica schists and garnet-mica schists. While kyanite crystals display more than 6 cm sizes, garnet crystals vary 1-2 cm in sizes (Kayhan 1991). Garnet mica schists are seen rarer than the other one. Biotite, quartz and plagioclases are determined as main minerals in the microscopical investigations. Biotites are generally hybidioblastic to xenoblastic in forms and show brownish pleochroisms (Plate I - Figure 3). They are affected from deformations and in some thin sections are observed as altered to chlorite and hydrobiotite (Plate 1 - Figure 4). Biotites are dark red to dark brown in colors when iron rich solutions affect the rocks, which caused opacitisation of the biotites. So, the biotites in ore samples are quite different from the other biotites. Biotites have sometimes inclusions. Muscovites appear in small amounts and are bended due to deformations.

Two kinds of quartz grains have been determined during microscopical studies. One type is fine grained quartz in mica schists and the other type is the coarser grains. Quartzs have xenoblastic textures and show undulating extinction.

In some thin sections, tourmaline, apatite, and zircon are observed as detritic grains, which are very fine grained and rounded. Rutiles are recognizable with their opaque and reddish colours. Opaque minerals take place parallel to schistosity.

Xenoblastic quartz are as veinlets with coarser grain sizes in ore samples. Biotites are also xenoblastic and bended. They are sometimes chloritized. Biotites exhibit dark red to dark brown colours due to iron bearing solutions and are fractured at these samples.

Kemer and Yılanlıkale Areas

Kemer area is located in the east, northeast of Zeytinlik Village and 9 km northeast of Ödemiş. It is on the road from Kemer to Yılanlıkale. The area is covered by mica schists and amphibolites which contains quartz-arsenopyrite mineralizations. These mineralizations are concordant with the schistosity of the rocks. The strikes and dips of the mineralizations are measured as N55E / 30SE and N80W / 76SW.

Amphibolites at Kemer area are lenticular and display massive character compared to mica schists caused by large scale boudinage. Amphibole, garnet, epidote, and plagioclase bearing amphibolites have dark greenish to blackish colours.

Amphiboles show medium to strong green pleochroism and identified as hornblendes. Xenoblastic hornblendes are fine grained and clustered.

Garnets are generally hypidiblastic to xenoblastic in textures. Both isotropic to anisotropic garnets are observed in thin sections. Some garnets are fracturated and epidotized due to hydrous solutions. Opaque minerals as inclusions occur in pinkish garnets which are supposed to be almadine type. In some sections, pinkish coloured garnets are accepted as secondary in origin and are found in veinlets.

Epidotes are also generally hypidioblastic to xenoblastic in forms. In some sections, the amount of epidotes are high (Plate 1 - Figure 6) which are determined as clinozoisites.

Plagioclases are fine grained and exhibit rounded crystals. Hypidioblastic to xenoblastic plagioclases present albite twinnings. They are brecciated and cataclastic.

Quartz are observed in very small amounts. Less than 5% amounts of quartzs display xenoblastic textures. Titanite (Plate 1 - Figure 5), rutile, zircon, and opaque minerals are accessories in thin sections.

Yılanlıkale area is located approximately 2 km's northeast of Kemer village and 3.5 km's southeast of Bozdağ. It crops out at the Kemer-Yılanlıkale road trench. Arsenopyrite mineralizations occur as fillings of veins and veinlets in the fault and fracture systems of mica schists. These mineralizations cut the rocks as stockworks. Quartz-arsenopyrite vein clusters have 1 cm to 50 cm thicknesses in a 120 m zone. Quartz lenses are squeezed and fractured due to chaotic tectonic events. The schistosities of mica schists are measured as N30-60W / 30-50W. The rocks in this area exhibit very similar mineralogical and petrographical features. Therefore, only minerals in ore samples and their features will be given in the following text.

In some ore samples, biotite flakes occur along the fractures and have brownish strong pleochroism. Biotites are lost their flaky appearances caused by ore solutions and due to hydrobiotitization and gained reddish colours.

Hypidioblastic muscovites are the products of biotite with 1-2% modal compositions. Quartz are generally as secondary veins. They are xenoblastic grains with mosaic textures. In ore rich zones, quartz are coarser than the other zones (Plate 1 - Figure 6).

Hypidiblastic plagioclases do not show albite type twinning and zonation. Porphyroblastic plagioclases are fractured and cracked with the effect of ore veins. Some of them are fracture fillings at ore zone sections. Titanite inclusions are observed in plagioclases. Shear fracturing in two directions are generally main features at this kind of ore samples. Due to fracturing, ore minerals are scattered to every directions in sections.

Small amount of amphiboles (hornblendes) as clusters, zircon bearing biotites as hypidioblasts to idioblasts, titanite and apatites, are the other minerals in these zones. Fractured and brecciated ores are silicified, carbonatized and scoroditized in most of the locations.

ORE MICROSCOPY

One sample (KM -3) from Kemer area, one sample (YK-2) from Yılanlıkale area and four samples (ZT-1, ZT-4, ZT-5, and ZT-10) from Zeytinlik area are ore microscopically investigated. The features of ore minerals are given below:

Observations are made in oil environment and under 250 magnifications. At the end of this chapter, a short summary of ore microscopy section of MTA-Italian project (SNIA TECHINT-RIMIN-GEOEXPERT ITALY, 1991) will be presented and correlations with this study will be done.

At ZT-1, ZT-4 and ZT-5 samples from Zeytinlik area, no scheelite mineral could be found in the polished sections, so investigations about the features of this mineral could not be given.

Arsenopyrite.- Main ore minerals of the sections are arsenopyrites up to 3.5-4 mm in sizes. They are cataclastic and generally idiomorphic. Due to tectonism, arsenopyrites are replaced by scorodites along their edges and cleavages (Plate 2 - Figure 1). In some parts of polished sections, arsenopyrite relicts are observable among scorodites. Some of them are as grains while others as disseminations. Disseminated ones show maximum 3 cm sizes. Sometimes, scorodites lie as zones between silicates and arsenopyrites. Fine magnetite and pyrite grains occur in arsenopyrites. Because of this feature, arsenopyrites are younger than magnetites and pyrites.

Scorodite.- They are secondary minerals as a result of weathering products of arsenopyrites. Green coloured scorodites are observed along the cracks of arsenopyrites. Arsenopyrite skeletals are formed as a result of replacement of scorodites at Yılanlıkale area. Colloform textures are the products of this event.

Native Gold.- Native gold grains vary in sizes up to 110 m x 250 m. In some parts of the sections, gold grains are scattered separately while in other parts as fine grained clusters. Native gold grain inclusions are in arsenopyrites or in scorodites. (Plate 2 - Figure 2) Gold grains fill the cracks of arsenopyrites in some places which indicate that those kind of gold grains are formed younger than arsenopyrites.

Pyrite.- Pyrites are observed mostly in arsenopyrites as subhedral to euhedral cataclastic crystals and sometimes as skeletons (Plate II - Figure 3). Pyrites are older than arsenpyrites because they are surrounded by arsenopyrites. This kind of pyrites are 0.3 - 0.4 mm in sizes. In some sections, growing traces can be seen between pyrites and marcasites. Some pyrites which are up to 1 mm sizes are formed as pseudomorphs of hexagonal pyrrhotite grains (Plate II - Figure 4). Pyrrhotite, marcasite and magnetite occur both in arsenopyrites and silicate minerals at host rock. Sometimes, chalcopyrites surround of pyrites.

Chalcopyrite.- Crystals up to 0.2 mm are formed together with arsenopyrites and as fillings of arsenopyrite cracks. In some places, they surround pyrites (Plate II - Figure 5). The youngest ore mineral in polished sections are beleived to be chalcopyrites. The arsenopyrite-chalcopyrite association are found especially at Kemer area and are 150 μm in sizes which are replaced by limonite and covellite (Plate II - Figure 6).

Other Opaque Minerals.- Rutiles are as tiny needles in 200 μm sizes and take place paralel to schistosity. Titanites are in very small amounts. Both opaque minerals are observed in biotites. On the other hand, rutiles after ilmenite occur in gangue minerals. Rounded-elipsoidal pyrrhotite grains form in amphibolites of Zeytinlik area.

SUMMARY OF ORE MICROSCOPIC STUDIES OF MTA-ITALIAN PROJECT

Elmacıgediği Area

First, pyrrhotite, arsenopyrite and scheelite paragenesis and at second stage chalcopyrite and marcasite association represent synmetamorphic mineralization. Marcasite could be an alteration product of pyrrhotite. The crystal sizes of pyrrhotite, pyrite, arsenopyrite and scheelite are less than 1 mm. Chalcopyrite and marcasites are finer than 0.1 mm in sizes. No free gold has been detected.

Zeytinlik Area

Euhedral arsenopyrites up to 2 cm in sizes exhibit elongated crystals. The grains are generally in silicates as poikiloblastic to porphyroblastic growths. Marcasite, stibnite and chalcopyrites are as intergrowths and fracture fillings.

Native gold occur both as inclusions in coarse grained arsenopyrites and at fine cracks which are filled by bismuthinite, chalcopyrite and quartz in arsenopyrites with less than 10 μm sizes.

Chalcopyrite are maximum 0.03 mm in sizes. They occur together with marcasite, bismuthinite and gold at small cracks.

Marcasites occur at the center of arsenopyrites with less than 0.5 mm. Primary pyrrhotites are possibly replaced by marcasites. They show sometimes intergrowths with chalcopyrites.

Scheelites up to 1 cm grains are as euhedral to subhedral porphyroblasts grown paralel to schistosity.

Yılanlıkale Area

Poikiloblastic and euhedral arsenopyrite crystals are brecciated due to secondary processes. Pyrite, pyrrhotite and chalcopyrite minerals occur at the cracks of arsenopyrites. Free gold and bismuthinite could not be seen. These minerals are as inclusions in less than 10 μm sizes.

ORE MICROSCOPIC CORRELATION AND INTERPRETATION

Arsenopyrites are euhedral and are found among silicate minerals and contain marcasite and chalcopyrite crystals at cracks and fractures of arsenopyrites. These features are the main similarities between this study and MTA-Italian Project. New finding at this study is that arsenopyrites occur both as grains and disseminations. They are younger than magnetites and pyrites and cataclastic and also scoroditized. For gold grains, they occur in arsenopyrites and at their cracks. This observation is the same at both studies. On the other hand, in this study, native gold grains are observed both separately and clustered, vary up to 250 μm in sizes and are found as free gold grains in scorodites.

Pyrites are found in the polished sections of this study, on the contrary marcasites are observed during MTA-Italian Project.

Bismuthinite, scheelite and stibnite are determined at MTA-Italian Project.

If all ore paragenesis data are interpreted all together :

1) Formation sequence of ore minerals from older to younger :

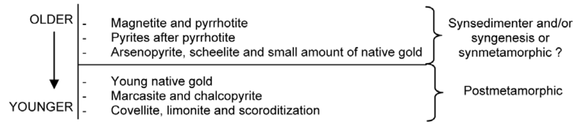

2) Euhedral arsenopyrites and their concordance to schistosity at Zeytinlik and Elmacıgediği areas are characteristics of this study. Vein type ore mineralizations and no ore mineral association which are seen at other areas, are observed at Yılanlıkale area should look like to indicate a late stage mobilization.

GEOCHEMISTRY

MAJOR AND TRACE ELEMENT ANALYSES AND EVALUATIONS

According to results of petrographical studies, 11 representative samples are selected from different zones of every area and chemically analysed. 7 samples from Zeytinlek area, 2 from Elmacıgediği area, 1 from Kemer and 1 from Yılanlıkale area belong to analysed samples. Analytical results from MTA-Italian Project samples are also used for correlations. Rock descriptions and analytical data are given at Table 1, 2, 3, 4, 5, and 6.

Elmacıgediği Area

All major oxide analyses are concordance with each other at amphibole schist samples. But at the sample named amphibole schist - amphibolite (EG-2a), SiO_2 content is a little bit lower, Fe_2O_3 content is higher. Analytical results of ore bearing sample (7579) are very similar to rock sample, which can be explained by low amount of ore. On the other hand, higher Fe_2O_3 content could be related to ore minerals. In addition, the similarities of major oxides with amphibolite or amphibole schists should point out that ore bearing solutions from their host rocks.

Trace element contents given on Table 4 were difficultly interpreted with the MTA-Italian Project

Table 1- Descriptions of analysed samples collected from study area

Sample Number	Locality	Description
EG-2a	Elmacıgediği	Garnet-amphibole schist-amphibolite contact
EG-6	Elmacıgediği	Amphibole schist
KM-1	Kemer	Ore sample (arsenopyrite)
YK-2	Yılanlıkale	Arsenopyrite ore (concentration)
ZT-1	Zeytinlik	Ore sample (arsenopyrite)
ZT-2	Zeytinlik	Biotite-muscovite-gaarnet-staurolite schist
ZT-3	Zeytinlik	Biotite-muscovite schist
ZT-4	Zeytinlik	Ore sample (arsenopyrite)
ZT-5	Zeytinlik	Ore sample (arsenopyrite)
ZT-6	Zeytinlik	Muscovite-biotite schist
ZT-10	Zeytinlik	Ore sample (arsenopyrite)

Table 2- Descriptions of analysed samples collected during MTA-Italian Project studies

	Sample Nr.	Locality	Description
MTA-Italian Joint Venture Project	7579	Elmacıgediği	Ore sample (arsenopyrite)
	8368	Elmacıgediği	Amphibole schist
	8369	Elmacıgediği	Amphibole schist
	TR-M-10	Yılanlıkale	Arsenopyrite ore (compiled sample)
	8381	Yılanlıkale	Ore sample (arsenopyrite)
	8414	Yılanlıkale	Arsenopyrite ore (concentration)
	8415	Yılanlıkale	Ore sample (arsenopyrite+quartz vein)
	7541	Zeytinlik	Quartz vein (Pyrite-arsenopyrite-wolframite)
	7544	Zeytinlik	Schist
	7545	Zeytinlik	Schist
	7548	Zeytinlik	Schist
	8375	Zeytinlik	Mica schist
	8378	Zeytinlik	Prasinite (meta volcanite)
	8426	Zeytinlik	Garnet amphibolite
	8429	Zeytinlik	Garnet – mica schist
	8432	Zeytinlik	Biotite gneiss
	8433	Zeytinlik	Mica schist
	8441	Zeytinlik	Garnet amphibolite
	TR-M-9	Zeytinlik	Arsenopyrite ore (compiled sample)
	TR-Au-Z1	Zeytinlik	Arsenopyrite ore (compiled sample)

samples due to their low detection limits of analyses. But by the comparison of 7579 sample to EG-2a and EG-6 samples, most of the results exhibit great similarities, except W, Mo, Cu, As, Sb, Au and Ni contents. It indicates that ore bearing samples and amphibolite / amphibole schists have similar trace element contents. Above given elements are connected with ore mineralizations.

High value of W at 7579 sample points out scheelite presence. Cu and As contents are also very high in ore sample.

Table 3- Results of analysed samples collected from study area (analyses are made at ACME Analytical Lab., Canada by ICP-ES and MS method)

Sample Nr →	ZT-1	ZT-2	ZT-3	ZT-4	ZT-5	ZT-6	ZT-10	EG-2a	EG-6	KM-1	YK-2
SiO_2(%)	45.74	61.64	62.68	42.02	61.64	62.54	46.75	55.85	64.54	43.76	4.17
Al_2O_3(%)	11.88	17.38	17.90	9.32	10.10	17.49	2.83	16.56	13.83	14.57	0.80
$Fe_2O_3^*$ (%)	16.94	6.95	4.91	21.45	10.63	4.49	22.29	8.49	6.15	13.29	37.97
MgO(%)	1.17	2.96	2.02	1.42	0.43	1.84	0.12	3.84	2.70	0.75	0.02
CaO(%)	3.82	1.59	1.03	2.54	3.08	1.15	0.41	8.72	7.30	21.02	0.17
Na_2O(%)	1.54	1.68	2.25	1.17	1.14	2.48	0.73	2.60	1.54	0.12	0.05
K_2O(%)	0.86	3.67	4.04	0.64	0.87	3.66	0.19	0.26	0.21	0.03	0.25
TiO_2(%)	0.27	0.95	0.44	0.23	0.39	0.44	0.22	0.96	0.92	0.57	0.07
P_2O_5(%)	0.55	0.19	0.02	0.62	0.18	0.05	0.11	0.68	0.25	0.08	0.04
MnO(%)	0.01	0.06	0.02	0.01	0.01	0.02	< .01	0.16	0.14	0.42	< .01
Cr_2O_3(%)	0.049	0.039	0.056	0.026	0.047	0.048	0.031	0.044	0.090	0.030	0.019
LOI	10.9	2.4	3.7	18.5	9.7	3.8	17.1	1.6	1.3	4.7	51.4
TOT/C	0.13	0.12	0.29	0.34	0.22	0.33	0.01	0.03	0.07	0.03	0.02
TOT/S	4.37	0.03	0.03	4.92	1.17	0.04	2.72	0.10	0.02	0.13	14.34
SUM	93.89	99.72	99.41	98.02	98.34	98.29	90.93	99.98	99.36	99.44	94.98

Sample Nr →	ZT-1	ZT-2	ZT-3	ZT-4	ZT-5	ZT-6	ZT-10	EG-2a	EG-6	KM-1	YK-2
Co(ppm)	10.2	9.9	12.7	11.4	2.2	9.9	27.1	21.7	19.9	11.1	30.0
Cs(ppm)	3.1	6.2	5.6	2.7	2.0	4.9	0.6	0.9	2.6	<0.1	0.7
Ga(ppm)	19.4	24.2	24.5	16.2	24.7	22.5	4.5	16.7	17.9	20.2	3.0
Hf(ppm)	2.8	5.4	4.2	2.2	3.7	4.0	1.4	4.8	5.2	2.6	<0.5
Nb(ppm)	5.7	13.8	8.4	4.2	7.6	7.8	3.2	11.9	12.0	13.4	1.1
Rb(ppm)	42.5	114.8	127.0	32.7	39.6	95.2	7.9	5.0	5.4	0.6	9.3
Sn(ppm)	<1	4	3	<1	3	3	2	4	8	25	<1
Sr(ppm)	446.8	264.1	209.6	235.6	501.0	204.3	195.0	356.6	283.6	205.5	30.4
Ta(ppm)	0.3	1.0	0.6	0.3	0.5	0.6	0.3	0.9	0.8	0.9	<0.1
Th(ppm)	5.5	10.3	9.6	5.8	11.1	10.4	1.9	9.1	7.4	17.4	1.0
U(ppm)	3.8	3.3	7.4	3.4	5.3	4.5	0.4	3.6	2.2	4.6	0.1
V(ppm)	102	124	141	77	68	131	24	94	71	140	27
W(ppm)	11.8	3.2	5.9	71.3	4005.4	15.2	14.4	2.7	4.8	3.5	18.6
Zr(ppm)	98.0	193.4	144.3	81.0	139.4	130.8	42.6	176.2	168.7	88.1	11.9
Y(ppm)	40.3	34.4	25.1	24.0	30.6	29.2	6.9	38.2	34.6	49.7	1.1
Mo(ppm)	5.8	0.8	8.5	4.4	12.1	10.3	4.5	1.3	1.3	0.7	2.7
Cu(ppm)	70.9	40.3	115.4	56.3	158.0	45.2	1.6	47.3	4.7	74.5	3.2
Pb(ppm)	11.5	3.8	8.9	6.7	18.3	7.6	2.0	4.0	5.2	8.7	2.6
Zn(ppm)	18	56	112	24	15	83	4	49	38	18	4
Ni(ppm)	979.1	975.7	1430.9	464.7	765.6,	1062.9	926.8	1430.0	2337.2	829.2	362.9
As(ppm)	>9999	77.4	709.4	>9999	6938.4	2233.2	>9999	467.5	570.4	1102.9	>9999
Cd(ppm)	0.1	< .1	0.5	0.1	0.1	0.2	< .1	0.4	0.3	0.2	< .1
Sb(ppm)	58.2	0.3	0.6	79.7	2.6	1.3	147.7	0.6	0.5	1.1	103.3
Bi(ppm)	18.7	0.3	0.9	23.9	19.5	0.9	231.4	0.6	4.7	1.9	13.0
Ag(ppm)	0.6	0.2	0.5	0.9	0.7	0.3	1.7	0.5	0.3	1.1	0.2
Au(ppm)	6.17	3	0.01	8.48	2.92	0.12	86.33	0.15	0.18	0.31	4.13
Hg(ppm)	0.01	0.01	0.02	0.18	0.64	0.23	0.09	0.01	0.01	< .01	0.21
Tl(ppm)	0.3	0.5	0.5	0.2	0.2	0.4	0.1	< .1	< .1	< .1	< .1
Se(ppm)	10.6	0.5	1.6	15.2	7.6	2.7	18.2	0.5	< .5	0.7	29.1

* Total iron as Fe_2O_3.

Table 4- Results of major oxide analyses of the samples collected during MTA-Italian Project studies.

Sample Nr →	7579	8368	8369	7541	7544	7545	7548	8375	8378	8426	8429	8432
SiO_2(%)	59.06	63.50	59.60	56.62	61.90	59.60	66.00	60.70	51.50	47.80	63.50	68.30
TiO_2(%)	0.82	0.93	0.94	0.35	0.49	0.98	0.83	0.51	0.31	3.00	1.14	0.87
Al_2O_3(%)	11.74	15.10	18.90	16.08	18.29	18.50	14.90	18.70	4.50	15.60	15.90	15.00
$Fe_2O_3^*$(%)	10.58	5.82	7.70	7.80	5.39	6.34	5.63	4.65	21.00	15.20	7.31	3.51
MnO(%)	0.08	0.21	0.10	0.11	0.12	0.10	0.08	0.05	-	0.19	0.10	0.02
MgO(%)	2.25	2.41	4.07	2.63	2.48	2.68	2.01	2.13	0.36	5.40	2.67	1.88
CaO(%)	5.12	6.66	1.15	9.28	2.43	1.81	2.25	1.34	0.54	7.14	2.21	2.30
Na_2O(%)	n.a	2.79	2.43	n.a	4.52	1.04	2.43	2.62	1.27	2.41	3.61	3.71
K_2O(%)	<0.02	0.10	3.42	0.13	2.32	4.03	1.88	3.80	1.68	1.31	2.32	2.44
P_2O_5(%)	0.29	0.40	0.23	0.69	0.26	0.19	0.21	0.09	0.17	0.51	0.31	0.12
LOI	n.a	0.90	2.10	n.a	2.50	2.50	1.60	4.70	19.80	1.80	1.10	2.00
SUM	98.14	98.80	100.80	98.08	100.88	97.95	97.85	99.80	98.60	100.60	100.10	100.60

Örnek No →	8433	8441	TR-Au-Z1	TR-M-9	8381	8414	8415	TR-M-10
SiO_2(%)	69.30	42.20	45.07	39.55	37.81	2.26	95.16	11.01
TiO_2(%)	0.85	5.04	0.26	0.24	0.18	0.09	0.03	0.15
Al_2O_3(%)	14.80	13.80	10.27	9.76	4.81	1.85	<1	<1
$Fe_2O_3^*$(%)	4.99	17.20	18.04	20.21	30.39	44.99	4.42	34.51
MnO(%)	0.05	0.14	<0.02	<0.02	<0.02	<0.02	<0.02	<0.02
MgO(%)	1.78	9.22	1.69	0.85	<0.50	0.89	<0.50	<0.50
CaO(%)	0.96	9.79	3.04	2.65	<1	3.49	<1	<1
Na_2O(%)	2.80	0.98	n.a	n.a	n.a	n.a	n.a	N.a
K_2O(%)	2.65	0.27	0.93	0.91	0.86	0.18	<0.02	0.2
P_2O_5(%)	0.16	0.42	0.39	0.58	0.07	0.11	0.03	<0.1
LOI	2.00	1.10	n.a	n.a	n.a	n.a	n.a	N.a
SUM	100.50	100.10	101.21	102.08	85.71	60.58	110.22	92.04

* Total iron as Fe_2O_3,- Below the dedection limit, n.a : not analysed.

Zeytinlik Area

SiO_2 contents of ore samples (ZT-1, ZT-4 and ZT-10) compiled from area are lower than 45% which are also lower than the mica schist's. On the other hand, ZT-5 sample has 61% SiO_2 value and similar to mica schists. Petrographical descriptions of ZT-5 sample also indicate mica schists. Al_2O_3 contents in ores and close to ore zones at ZT-1, ZT-4 and ZT-5 samples vary between 9-10%, but samples from mica schists (ZT-2, ZT-3 and ZT-6) exhibit more than 17% Al_2O_3 contents. ZT-10 ore sample has the lowest Al_2O_3 value with 2.83%. MgO contents of ore samples, except ZT-10 sample, vary between 1 to 4%. Mica schists have more the 1.84% MgO values. This indicates a 1 to 2% differences between ore samples and mica schists. Ore samples contain 2,5 - 3,8% CaO contents again except ZT-10 sample, while mica schists have 1 - 1,6% CaO values. P_2O_5 contents of ore samples are more than other samples. K_2O values of ore samples are less than 0.87%, while mica schist have higher contents.

Table 5- Results of trace element analyses of the samples collected during MTA-Italian Project studies.

Sample Nr →	7579	8368	8369	7541	7544	7545	7548	8375	8378	8426	8429	8432
V(ppm)	66.9	n.a	n.a	110.2	n.a	n.a	n.a	n.a	n.a	n.a	n.a	N.a
Co(ppm)	14	12	14	25.1	31	-	14	-	-	11	17	47
Ni(ppm)	45.5	37	60	200.9	90	10	43	13	-	24	43	71
Sn(ppm)	<16	-	-	<16	-	-	-	-	-	-	-	-
W(ppm)	851.5	n.a	n.a	16	n.a	n.a	n.a	n.a	n.a	n.a	n.a	n.a
Mo(ppm)	7.7	n.a	n.a	<4	n.a	n.a	n.a	n.a	n.a	n.a	n.a	n.a
Cu(ppm)	510.3	30	32	84	-	-	-	15	75	97	18	39
Pb(ppm)	<20	-	-	56.4	-	-	-	18	-	-	-	-
Zn(ppm)	43	31	164	575.9	234	116	138	76	-	102	109	63
As(ppm)	32826	-	-	225	-	-	-	105	5910	-	-	68
Sb(ppm)	20	n.a	n.a	<20	n.a	n.a	n.a	n.a	n.a	n.a	n.a	n.a
Bi(ppm)	<20	n.a	n.a	<20	n.a	n.a	n.a	n.a	n.a	n.a	n.a	n.a
Hg(ppm)	<0.1	n.a	n.a	<0.1	n.a	n.a	n.a	n.a	n.a	n.a	n.a	n.a
Au(ppm)	0.34	n.a	n.a	0.01	n.a	n.a	n.a	n.a	n.a	n.a	n.a	n.a
Ag(ppm)	<1.0	n.a	n.a	<1	n.a	n.a	n.a	n.a	n.a	n.a	n.a	n.a
Ba(ppm)	78.8	85	556	103.9	483	1090	312	809	300	265	608	869
Rb(ppm)	n.a	-	131	-	100	136	84	136	98	51	86	68
Sr(ppm)	443.5	302	250	727.4	334	181	205	280	232	300	243	177
Li(ppm)	21.2	n.a	n.a	55.1	n.a	n.a	n.a	n.a	n.a	n.a	n.a	n.a
Nb(ppm)	11.8	10	-	9.2	-	10	-	10	-	18	10	-
Zr(ppm)	192.4	228	199	123	185	239	235	200	124	230	371	263
Y(ppm)	36.1	33	33	32.6	28	47	44	39	-	30	33	24
Th(ppm)	n.a	-	-	n.a	-	-	-	-	27	-	-	-
U(ppm)	n.a	-	-	n.a	-	-	-	-	-	-	-	-
Cr(ppm)	69.1	46	67	54.8	73	100	88	80	-	34	94	72
Cd(ppm)	<2.0	n.a	n.a	4.7	n.a	n.a	n.a	n.a	n.a	n.a	n.a	n.a

Sample Nr →	8433	8441	TR-Au-Z1	TR-M-9	8381	8414	8415	TR-M-10
V(ppm)	n.a	n.a	90.7	103.3	17.9	56.6	4.5	36.3
Co(ppm)	-	54	13.8	27.4	12.9	27.4	2.2	30.6
Ni(ppm)	18	94	56.2	42	6.1	25.3	<6	15.8
Sn(ppm)	-	-	<16	<16	17.8	16.4	20.8	<16
W(ppm)	n.a	n.a	1669.4	1050.2	454	<16	<16	<16
Mo(ppm)	n.a	n.a	20.9	21.1	<4	<4	<4	23.4
Cu(ppm)	60	57	75.1	72.8	3.4	5.1	4.1	3.9
Pb(ppm)	-	-	20	28.1	<20	<20	<20	<20
Zn(ppm)	75	231	59.3	60.9	28.5	63.2	10.4	60.9
As(ppm)	-	-	113000	150000	50000	50000	17000	287000
Sb(ppm)	n.a	n.a	89.3	115	90.3	113.5	32.1	137.5
Bi(ppm)	n.a	n.a	21.1	47	<20	<20	<20	38
Hg(ppm)	n.a	n.a	5	<0.1	5.1	4.8	0.3	<0.1
Au(ppm)	n.a	n.a	4.5	17	1.9	2.2	0.3	6.7
Ag(ppm)	n.a	n.a	<1	1	<1	<1	<1	<1
Ba(ppm)	872	140	236.7	244	308.2	599.7	58.8	735.9
Rb(ppm)	76	10	n.a	n.a	n.a	n.a	n.a	n.a
Sr(ppm)	180	105	347.9	302.2	95.9	395.7	9.3	120
Li(ppm)	n.a	n.a	7.8	17.1	<4	<4	<4	6.9
Nb(ppm)	-	22	3.9	5.3	6.3	<2	<2	2.7
Zr(ppm)	212	190	106.7	98.1	210.1	9.1	<2	15.6
Y(ppm)	21	15	21.2	22.7	3.7	2.8	<1	2.2
Th(ppm)	-	-	n.a	n.a	n.a	n.a	n.a	n.a
U(ppm)	-	-	n.a	n.a	n.a	n.a	n.a	n.a
Cr(ppm)	65	150	42	78.4	18.1	21.4	9.9	8.2
Cd(ppm)	n.a	n.a	<2	<2	<2	<2	<2	<2

- Below the dedection limit, n.a : not analysed.

Table 6- The symbols representing the samples on the graphics

Rock types	Description	Symbol	
		This study	Ital.Proj.
Amphibole bearing rocks	Amphibole schists and amphibolites	▲	△
Schists	All schist samples (except amphibole schists)	◆	◇
Ore samples	All ore samples	■	□
Gneiss	Biotite gneiss	-	○
Vein	Quartz vein	-	x
Prasinite	Meta volcanite	-	+

- Not observed in this study

SiO_2 contents of ore samples and amphibolites are lower than mica schists at MTA-Italian Project samples. TiO_2 values are high at amphibolites and Fe_2O_3 contents are also high at amphibolites, ore samples and meta volcanite (prasinite). Amphibolites contain higher amount of MgO. Major oxide analytical results of MTA-Italian Project samples are in concordance with this study.

At samples ZT-1 to ZT-6 in Table 3, higher amount of As, Sb, Bi, Au and Se point out ore zones. As contents of ore samples (ZT-1, ZT-4, ZT-5 and ZT-10) are higher than 7000 ppm. Mica schists have 77 - 2200 ppm As values. Sb, Bi and Se contents of ore samples are higher than mica schists.

When all samples collected from Zeytinlik area are interpreted, Ni contents exhibit heterogeneties. Ni contents of mica schists vary between 10 and 1463 ppm and are higher than ore samples. W value is high only with 4000 ppm at ZT-5 sample. On the other hand, channel samples (TR-Au-Z1 and TR-M-9) from MTA-Italian Project exhibit a little bit high W contents. At these samples, As values with 113000 ppm and 150000 ppm are very high.

At ore samples, Au contents vary 3 to 9 ppm. Only ZT-10 sample contain 86,33 ppm gold value. In connection with Au content, this sample has higher contents of Ag, Sb, and Bi but lower contents of Zn, Rb, Cs, Ga, Zr, Y, Th, U and Sc when compared with other samples. On the other hand, V, Co, W, Mo and Cu contents of this sample are higher than other ore samples but very close to mica schists.

At all major oxide versus SiO_2 diagrams, amphibole bearing rocks, schists and ore samples plot at different areas (Figure 2).

At TiO_2, Al_2O_3, MnO and MgO versus SiO_2 diagrams, major oxide contents of ore samples are lower than the contents of schists and amphibole bearing rocks. Total Fe_2O_3 and P_2O_5 values are similar both at ore samples and amphibole bearing rocks. No discrimination could be seen at rocks due to Na_2O and K_2O contents. TiO_2, MnO and MgO contents of amphibole bearing rocks are clearly higher than ore samples and schists. Total Fe_2O_3 contents of amphibole bearing rocks and ore samples look like very similar (Figure 2).

At a few samples collected from the rocks which are parallel to schistosity at Zeytinlik area, trace element contents are evaluated statistically e.g. Cluster analyses. According to this method three main association have been determined. First one is Cr-Ni association, second ore is rep-

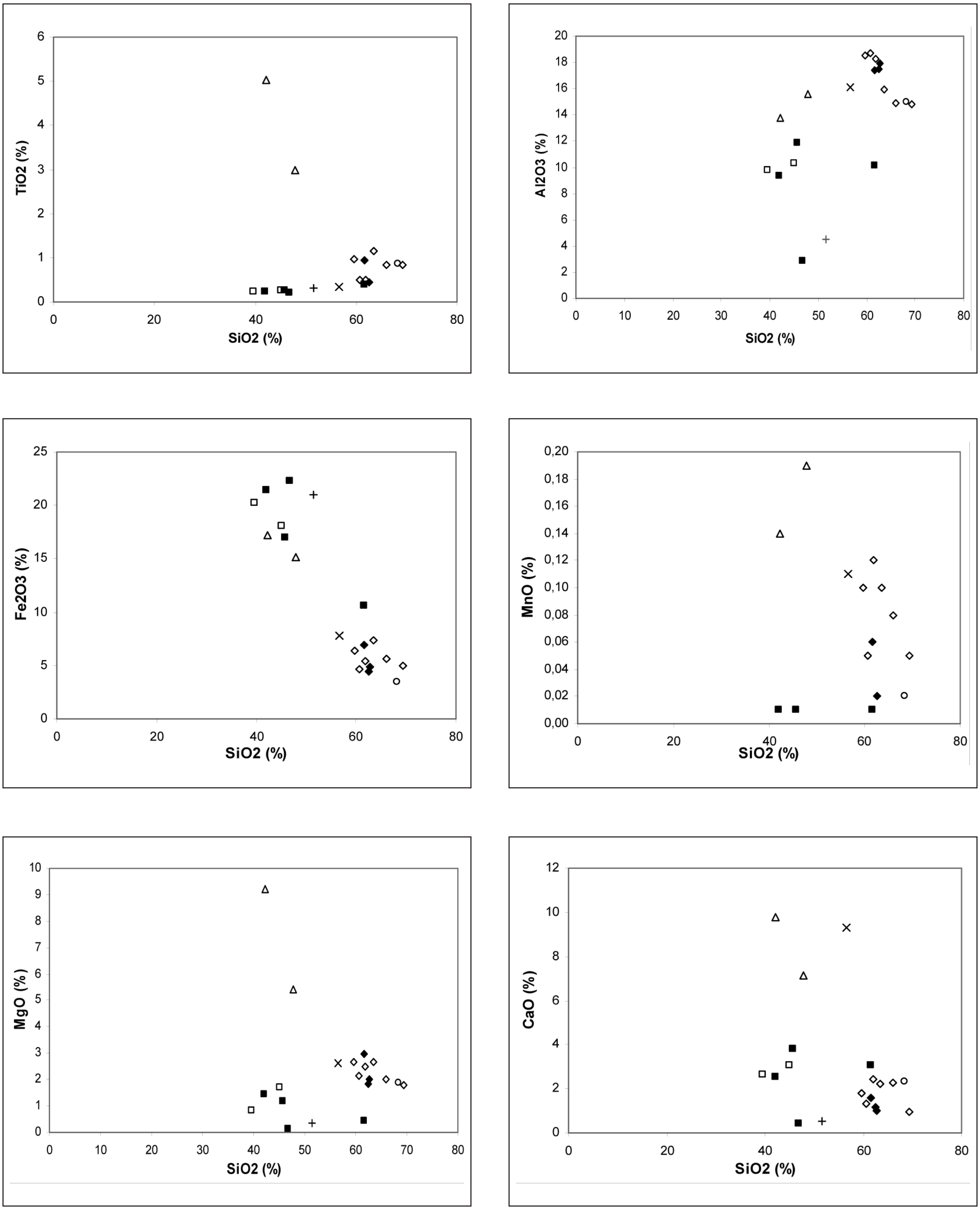

Figure 2- Harker diagrams (SiO_2 versus major oxides).

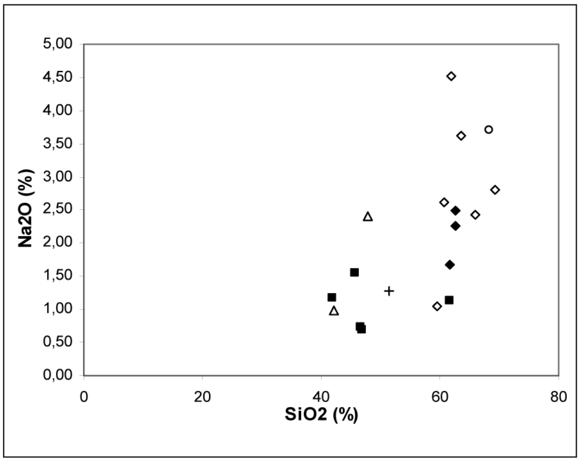

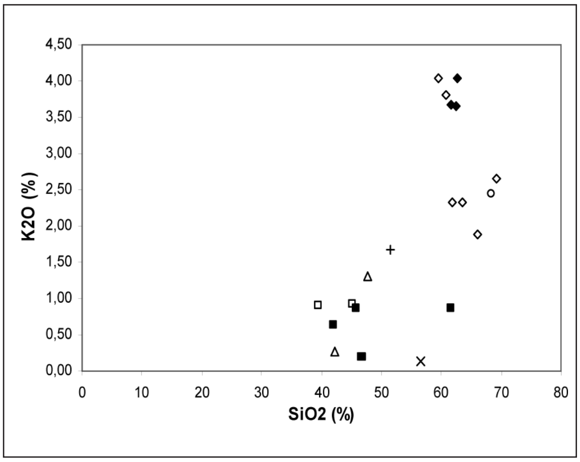

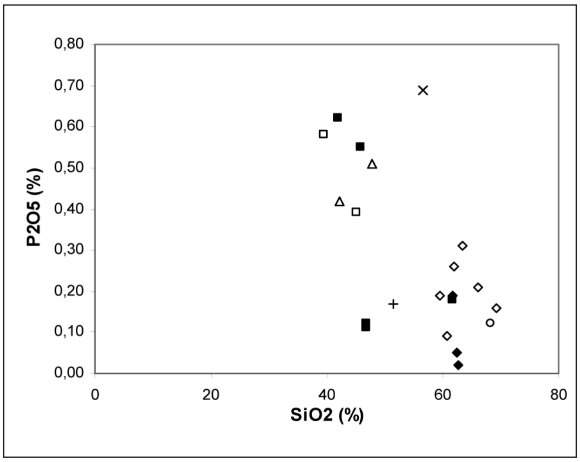

Figure 2- Continue

resented by U-V-Cu-Mo-Pb-Th-Ba association. Third association includes Au-Ag-Bi-Sb-Se elements (more detailed information, see Akıska 2003).

Kemer-Yılanlıkale Areas

All samples compiled from these areas are either ore-rich samples or channel samples. SiO_2 contents of analysed samples verify it. 95.16% SiO_2 content of sample 8415 points out arsenopyrite bearing quartz vein. On the other hand, 8414 and YK-2 samples contain only 2-4% SiO_2. These samples are rich in arsenopyrite and therefore SiO_2 contents are low. Except than 8415 sample which represents quartz vein, Fe_2O_3 content of all samples are high. SiO_2, Al_2O_3 and CaO contents of KM-1 sample are higher than other samples which can be interpreted that this sample represent host rock with ores. K_2O value of KM-1 sample is low. But with 21% of CaO content of this sample indicate an extraordinary composition of it. High content of CaO can be regarded to garnet and epidote minerals due to petrographical studies.

Due to trace element values, KM-1 sample shows special contents. V, Ni, Cu, Nb and Y and also possibly U and Th values are higher but W, Sb, Bi and Hg contents are lower than other samples. W content of 8381 sample is 454 ppm which point out presence of scheelite.

When arsenopyrite ore concentrations of TR-M-10 and YK-2 samples are compared to each other, except Ba and Sr contents, all trace element values are in concordance with each other. As is 287000 ppm at TR-M-10 sample and is also high at YK-2 sample. Au contents of all samples vary between 0,3 and 6,7 ppm.

Another characteristic feature of this area is that Sn contents, except than YK-2 sample, are higher than 16 ppm. Sb values are higher than 32,1 ppm which reachs up to 137 ppm with the KM-1 sample exception.

Rare Earth Element Analyses

The REE analytical results of all samples from Elmacıgediği, Zeytinlik, Kemer and Yılanlıkale areas are given at Table 7. Additionally the average contents of the crust, and basalt and shale are added to that table. Using all the data, the condrite normalized values are plotted into the diagram of Sun and Mc Donough (1989) in figure 3.

Table 7- Results of the rare earth element analyses at Elmacıgediği, Zeytinlik, Kemer and Yılanlıkale samples and average values of the rare earth elements in the crust, basalt and shale samples.

Sample Nr	EG-2a	EG-6	KM-1	YK-2	ZT-1	ZT-2	ZT-3	ZT-4	ZT-5	ZT-6	ZT-10
La	46.9	33.1	8	1.8	48.1	39.7	29.1	36.2	46.1	32.2	6.3
Ce	91.6	62.9	27.4	3.2	85.6	75.9	52.1	59.8	75	57.3	10.3
Pr	10.78	7.87	5.22	0.39	10.76	9.12	6.75	7.4	8.98	7.64	1.13
Nd	54.2	37	35.4	2	46.9	39	28	34.1	38.8	35.1	4.7
Sm	10	6.6	8.1	0.3	8.6	8.1	5.7	6.5	6.6	6.8	0.6
Eu	2.53	1.65	2.65	0.08	2.75	1.44	0.99	2.12	2.93	1.31	0.16
Gd	9.17	5.85	7.73	0.39	7.97	6.3	4.06	5.61	5.42	5.4	0.45
Tb	1.45	1.03	1.5	0.05	1.29	1.11	0.75	0.82	0.99	1.03	0.15
Dy	6.36	5.24	8.35	0.2	6.45	5.82	3.63	3.87	4.24	5.27	0.95
Ho	1.32	1.09	1.67	0.07	1.26	1.09	0.79	0.74	0.97	0.98	0.25
Er	3.53	3.38	4.8	0.13	3.65	3.39	2.4	1.93	2.77	2.77	0.71
Tm	0.54	0.5	0.71	<0.05*	0.5	0.54	0.39	0.32	0.41	0.44	0.13
Yb	3.99	3.27	4.93	0.15	3.56	3.4	2.57	2.3	2.94	3.05	0.8
Lu	0.52	0.47	0.62	0.03	0.56	0.56	0.41	0.4	0.47	0.4	0.12

	CRUST**	BASALT**	SHALE**
La	35	10	40
Ce	70	30	70
Pr	8	4	9
Nd	30	20	30
Sm	7	5	7
Eu	1,2	1,5	1,4
Gd	7	6	6
Tb	1	0,8	1
Dy	6	4	5
Ho	1,5	1	1,5
Er	3,5	3	3,5
Tm	0,5	0,5	0,6
Yb	3,5	2,5	3,5
Lu	0,6	0,5	0,6

* REE element values under the detection limits of the instrument are used in diagrams in order to provide the togetherness of all values.

** Krauskopf 1989, p,545 (In this book, the basalt values includes the basalt, diabase and gabbro values)

Table 8- The rock types of the samples in Table 7.

Samp. Nr	Location	Rock Types
EG-2a	Elmacıgediği	Garnet-amphibole schist-amphibolite contact
EG-6	Elmacıgediği	Amphibole schist
KM-1	Kemer	Ore (arsenopyrite)
YK-2	Yılanlıkale	Arsenopyrite ore (concentration)
ZT-1	Zeytinlik	Ore (arsenopyrite)
ZT-2	Zeytinlik	Biotite-muscovite-garnet-staurolite schist
ZT-3	Zeytinlik	Biotite-muscovite schist
ZT-4	Zeytinlik	Ore (arsenopyrite)
ZT-5	Zeytinlik	Ore (arsenopyrite)
ZT-6	Zeytinlik	Muscovite-biotite schist
ZT-10	Zeytinlik	Ore (arsenopyrite)

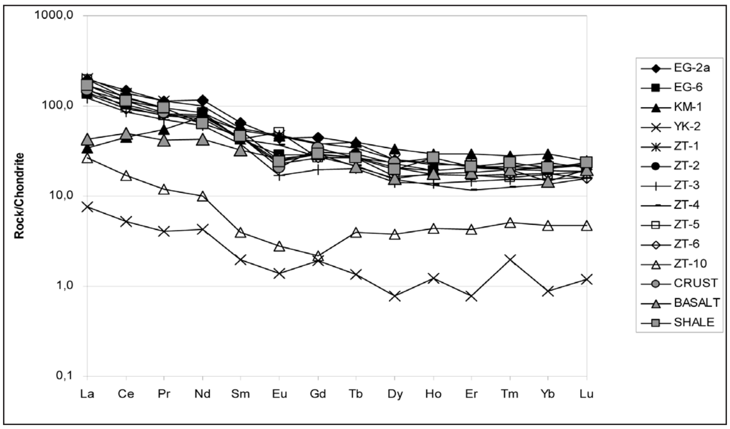

Figure 3- Chondrite normalized (Sun ve McDonough, 1989) spider diagrams of the samples in table 7.

According to these diagrams, the contents of all samples exhibit very close trends with crust and shale averages and very similar with basalt averages. Only YK-2 sample, which represents ore mineral concentrations, have another trend because of lack of silicate minerals. ZT-10 sample shows another trend which is poor in silicate minerals, but rich in iron ratio and gold (86 ppm) due to hydrothermal effects.

DISCUSSION AND CONCLUSIONS

Data, findings and results gained from investigations at Zeytinlik, Elmacıgediği, Yılanlıkale and Kemer areas are given below :

Due to field and laboratory studies, amphibolite and/or amphibole schists have been determined and ore zones are found either in these rocks or in their close vicinities in all areas. Arsenopyrite crystals are generally coarse grained and occur parallel to the schistosity. Scheelite sometimes accompany to arsenopyrites. Some amount of Sb, Bi and Ag enrichments are determined in the ore zones. Amphibolites at MTA-Italian Project are described as orthoamphibolites, i.e. magmatic in origin. This data is verified at our samples geochemically by high Ti, Cr and Ni contents. In all areas, both arsenopyrite ores parallel to schistosity and cutting across all the rocks have been observed. Depending upon all these data and concordance of ores with the schistosity, it can be postulated that mineralizations occured in association of various element incomes related to basic magmatism which comes to the basin during sedimentation. Basic solutions ceased with the time and an asidic stage with its solutions is dominated. All sedimentary and magmatic events occured synsedimentary and then metamorphosed. Further effects caused the mobilization of the ores. These effects could be the metamorphic stages and/or granitic intrusions. Trace element associations from Zeytinlik area could indicate basic magmatic rocks. Samples from Zeytinlik area are collected at zones which are parallel to schistosity. Cr-Ni associations are related to basic magmatic rocks, further U-V-Cu-Mo-Pb-Th-Ba association to asidic solution in comes to the basin. Final element association of Au-Ag-Bi-Sb-Se indicate mineralizations.

ACKNOWLEDGEMENTS

This study is a summary of the Master's Thesis of the first author at the Geological Engineering Department of Ankara University supervised by second and third authors. The authors acknowledge geological engineers Fahrettin Kayhan, Nevzat Karabalık and Dr.Ahmet Çağatay for their supports on the different stages of this study.

Manuscript received December 4, 2007

REFERENCES

Akıska, S. 2003. İzmir-Ödemiş yöresindeki metamorfik kayaçlar içerisinde bulunan altınlı arsenopirit damarlarının jeolojisi, jeokimyası ve kökeni. Yüksek lisans tezi, Ankara Üniversitesi Fen Bilimleri Enstitüsü, 101 s.

Andiç, T. 1992. Aydın-Denizli yöresi altın aramaları raporu. MTA Rapor No: 9521. Ankara.

Aydal, D. 2000. Altın ve jeolojisi, 82 s., Ankara.

Çağatay, A. and Eyüpoğlu, T. 1979. Batı Anadolu'daki antimonit-arsenopirit, zinober şeelit yatak ve zuhurlarının mineralojisi, kısa jeoloji incelemeleri ve elde edilen jenetik bulgular. JMO Bulletin Sayı:9 s. 51-62.

Dilek, S. and Kayhan, F. 1987. Menderes Masifi Ödemiş ve Çine asmasifleri arsenopirit mineralizasyonları raporu. MTA Report No: 8261. Ankara. (unpublished).

Gonca, Ş. 1992. Uşak-Eşme, Manisa-Kula, Manisa ve Uşak yöresinde altın aramaları maden jeolojisi raporu. MTA Report No:9520, Ankara (unpublished).

Kayhan, F. 1991. Ödemiş Asmasifinde (Menderes Masifi) ve yöresindeki altın mineralizasyonu raporu. MTA Report No:9350. Ankara (unpublished).

Krauskopf, K., B., 1989, Inroduction to Geochemistry, McGRAW-HILL INTERNATIONAL EDITIONS, Earth and Planetary Sciences Series, p.617.

Kuhns, R. J. 1988. The Golden Giant deposit, Hemlo, Ontario: geologic, and geochemical relationships between mineralization, alteration, metamorphism, magmatism and tectonism. PhD Thessis, Univ Minnesota 381 pp.

Önal, G., Yüce, A.E. and Karahan, S. 1986. Türkiye'de altın madenciliği, Yurt Madenciliğini Geliştirme Vakfı yayını, 173 s.

Sawkins, F. J. 1990. Metal deposits in relation to plate tectonics (Second Edition); (çeviri : Ünlü, T. ve Sayılı, İ.S., 366 s., 1999, Ankara).

SNIA TECHINT-RIMIN-GEOEXPERT ITALY, 1991. Hidrometallurjik Yöntemlerin Katkısıyla Batı Anadolu'da Değerli Metal ve Nadir Element Metallerinin çıkarılmasında Jeolojik ve Madencilik Araştırmaları. MTA Archive.

Strachan, D. M. and Moffett, R. 1985. Geology of the Lupin gold deposit, N.W.T. Preprint 11 NW Min Assoc 91st Annu Conv, Spokane.

Sun, S.S. and McDonough, W.F., 1989. Chemical and isotopic systematics of oceanic basalts: implications for mantle composition and processes. In: Saunders A.D. and Norry M.J. (eds.), Magmatism in ocean basins. Geol. Soc. London. Spec. Pub. 42, pp.313-345.

Uzkut, İ. 1977. Büyük Menderes-Gediz arasındaki arsenopirit yataklarının oluşumu ve altın-kobalt açısından önemi. Doçentlik Tezi, E.Ü.M.B.F., 92s.

PLATES

PLATE I

Figure 1 - Biotites including zircon inclusions in biotite-garnet schists (Bi: Biotite, Gr: Garnet, Zr: Zircon). Plane light.

Figure 2 - Strong green pleochroism exhibiting hornblendes in amphibolite (Hb: Hornblende, Gr: Garnet). Plane light.

Figure 3- Biotite flakes and garnet porphyroblasts in mica schists (Bi: Biotite, Gr: Garnet). Plane light.

Figure 4 - Chloritization of biotites in mica schists. (Bi: Biotite, Op: Opaque minerals, Kl: Chlorite). Plane light.

Figure 5 - Titanite grains surrounded by hornblendes and epidotes in amphibolites (Hb: Hornblende, Ep: Epidote, Sf: Titanite). Crossed polars.

Figure 6 - Coarse-grained quartzs in mica schists (K: Quartz, Op: Opaque minerals, Sk: Scorodite). Crossed polars.

PLATE - I

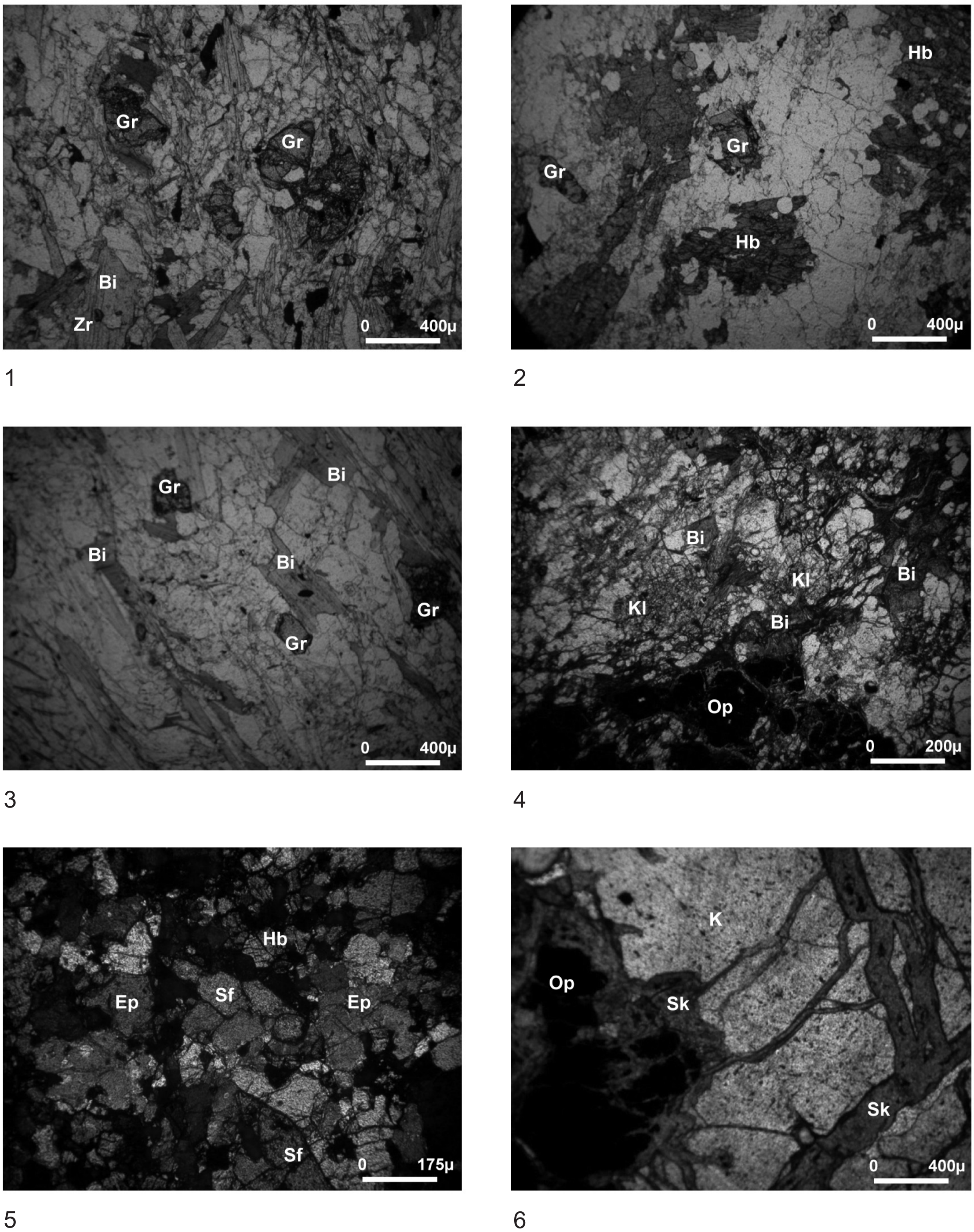

1 2 3 4 5 6

PLATE II

Figure 1 - Scorodites occured along the cleavages and fractures of arsenopyrites. Plane light.

Figure 2 - Coarse-grained native gold grains in scorodites (Sk: Scorodite, Au: Gold). Plane light.

Figure 3 - Pyrite, chalcopyrite and arsenopyrite association (Py: Pyrite, Kpy: Chalcopyrite, Asp: Arsenopyrite). Plane light.

Figure 4 - Pyrite and marcasites formed after hexagonal pyrrhotite (Py: Pyrite, Ma: Marcasite). Plane light.

Figure 5 - Chalcopyrite surrounded by pyrite grain and relicts of arsenopyrite Kpy: Chalcopyrite, Py: Pyrite, Asp: Arsenopyrite). Plane light.

Figure 6 - Chalcopyrites locked with arsenopyrites. Chalcopyrites are altered to covelline and limonite along its fracture (Asp: Arsenopyrite, Ko: Covelline, Li: Limonite, Kpy: Chalcopyrite). Plane light.

PLATE - II

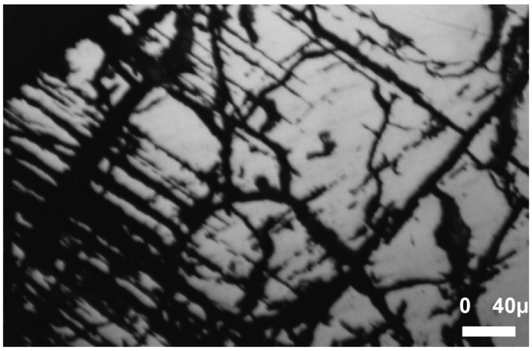

1

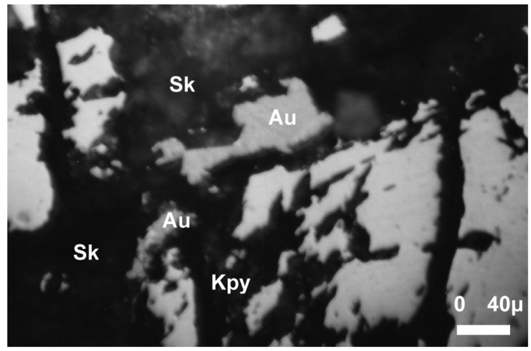

2

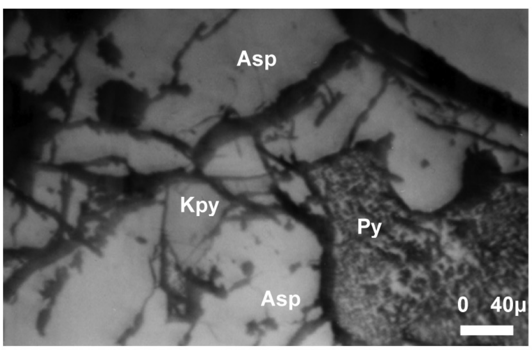

3

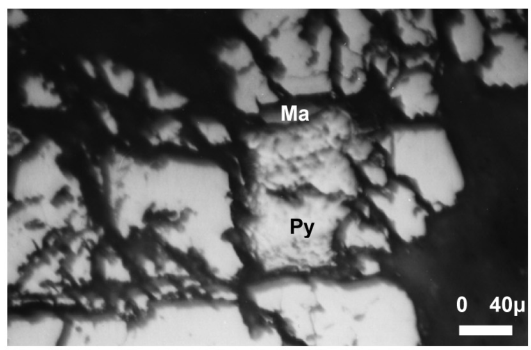

4

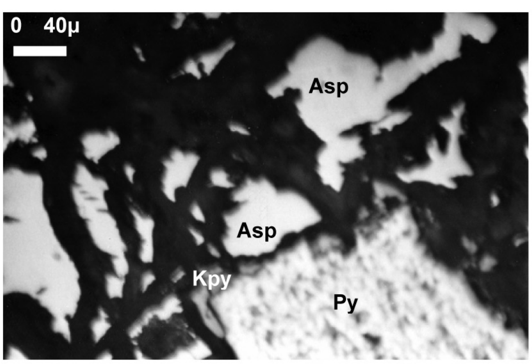

5

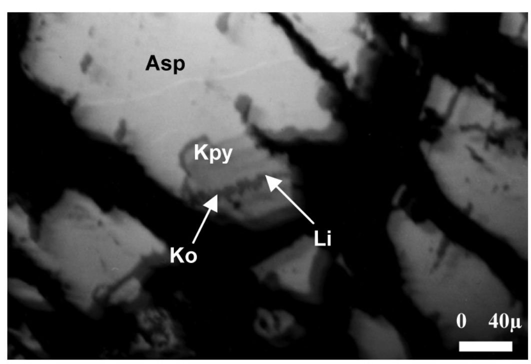

6

bos sayfa